



Short communication

B-site doping of lanthanum strontium titanate for solid oxide fuel cell anodes

David N. Miller*, John T.S. Irvine

School of Chemistry, University of St Andrews, North Haugh, St Andrews KY16 9ST, Scotland, United Kingdom

ARTICLE INFO

Article history:

Received 1 August 2010

Received in revised form

10 November 2010

Accepted 12 November 2010

Available online 1 December 2010

Keywords:

Perovskite

Strontium titanate

SOFC

Anode

ABSTRACT

In this study the properties of the compounds $\text{La}_{0.33}\text{Sr}_{0.67}\text{Ti}_{0.92}\text{X}_{0.08}\text{O}_{3+\delta}$ where $\text{X} = \text{Al}^{3+}, \text{Ga}^{3+}, \text{Fe}^{n+}, \text{Mg}^{2+}, \text{Mn}^{n+}$ and Sc^{3+} , have been investigated in the search for alternative solid oxide fuel cell anodes. The choice of dopant controls the structure, redox properties, conductivity and electrocatalytic properties of the compound.

© 2010 Elsevier B.V. All rights reserved.

1. Introduction

Doping of the cubic perovskite, strontium titanium oxide, has lead to a range of compounds that have shown potential for use in the anodes of solid oxide fuel cells [1–5]. Previous studies of these compounds have shown that conductivities as high as 5000 S cm^{-1} are possible in reducing conditions [1]. This high conductivity in reducing conditions makes them potentially useful as current collectors or as a replacement for nickel and other metals as the electronic conducting phase in composite anodes. Studies have also shown that some of these compounds exhibit catalytic properties that make them potential fuel oxidation catalysts [6–8].

In addition to their conductivity and catalytic properties these materials exhibit a number of other properties that make them suitable for use in fuel cell anodes. Studies have shown them to be chemically and thermally stable, tolerant to sulphur poisoning and redox cycling [1,9].

Previous studies have shown that by replacing Sr^{2+} on the perovskite A-site or Ti^{4+} on the perovskite B-site the properties of the titanate can be altered. Doping with 3+ ions on the perovskite A-site increases the oxygen stoichiometry beyond ABO_3 and increases the ease and amount of reduction of Ti^{4+} to Ti^{3+} increasing the conductivity. The trivalent lanthanum ion is a commonly used dopant for increasing the electrical conductivity of strontium titanate. Canales-Vazquez et al. have shown that La^{3+} doped SrTiO_3 can be used as the conducting phase in a fuel cell anode [9]. When stron-

tium titanate is doped with a higher valency cation, such as La^{3+} , the extra positive charge must be balanced by reduction of Ti^{4+} to Ti^{3+} , or by incorporating oxide ions into the structure beyond the ABO_3 stoichiometry. When the titanate is fired in reducing conditions the extra positive charge is accommodated by the reduction of Ti^{4+} . In oxidising conditions where Ti^{4+} cannot be reduced to Ti^{3+} , Canales-Vazquez et al. found that extra oxygen can be incorporated into the structure up to levels of about $\text{ABO}_{3.17}$ by the formation of short nanometre scale defects similar to the extended oxygen rich layers in $\text{La}_2\text{Ti}_2\text{O}_7$ [10].

Replacing the titanium on the perovskite B-site with other dopants has been shown to alter the catalytic properties as well as the conductivity. Properties can be further tailored by reducing the overall occupancy of the perovskite A-site. B-site dopants that have been previously investigated include manganese, cobalt, chromium, iron, gallium and scandium [3,6–8,11–13]. Of particular note are the results of Ruiz-Morales et al. where codoping on the B-site with Ga and Mn produced anodes comparable in performance to Ni–YSZ anodes [7].

Previous studies of doped lanthanum strontium titanates have concentrated on a single B-site dopant. In this study the structure, redox behaviour, conductivity and electrocatalytic properties of the compounds $\text{La}_4\text{Sr}_8\text{Ti}_{11}\text{XO}_{36+\epsilon}$ ($\text{La}_{0.33}\text{Sr}_{0.67}\text{Ti}_{0.92}\text{X}_{0.08}\text{O}_{3+\delta}$) where $\text{X} = \text{Al}^{3+}, \text{Ga}^{3+}, \text{Fe}^{n+}, \text{Mg}^{2+}, \text{Mn}^{n+}$ and Sc^{3+} will be compared.

2. Materials and methods

The compounds were prepared by traditional solid-state reaction. Stoichiometric amounts of high-purity (>99%) La_2O_3 , SrCO_3 , Mn_2O_3 , Ga_2O_3 , magnesium carbonate hydroxide pentahydrate,

* Corresponding author. Tel.: +44 1334 43844; fax: +44 1334 463808.
E-mail address: dnm7@st-andrews.ac.uk (D.N. Miller).

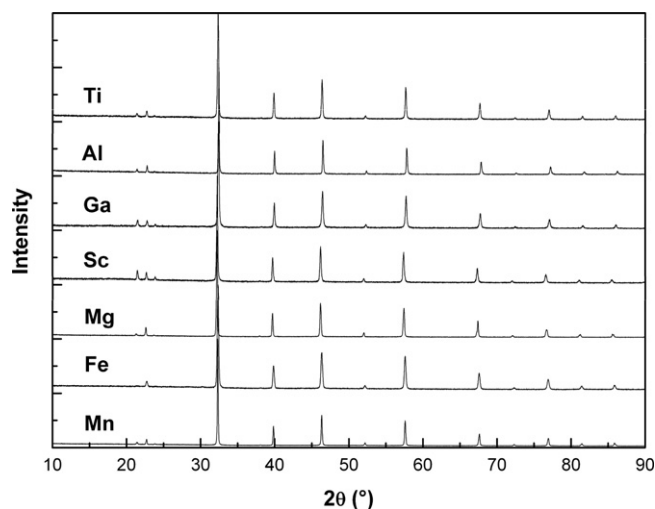


Fig. 1. X-ray diffraction trace of the compounds $\text{La}_4\text{Sr}_8\text{Ti}_{11}\text{XO}_{36+\epsilon}$ ($\text{X} = \text{Ti}, \text{Al}, \text{Ga}, \text{Fe}, \text{Mg}, \text{Mn}$ or Sc).

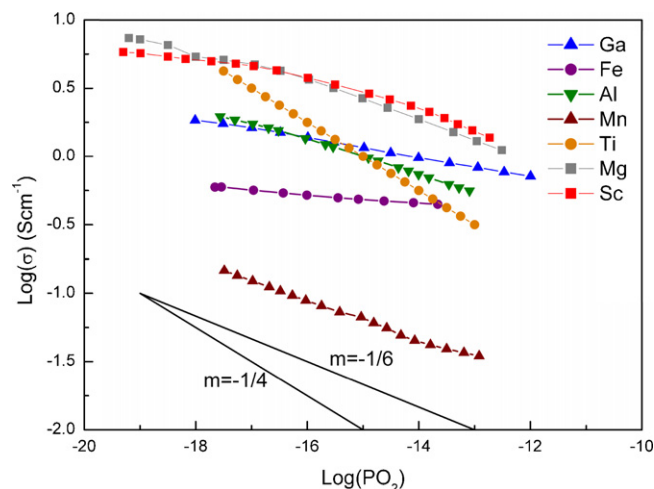


Fig. 3. Variation of the conductivity of $\text{La}_4\text{Sr}_8\text{Ti}_{11}\text{XO}_{36+\epsilon}$ ($\text{X} = \text{Ti}, \text{Al}, \text{Ga}, \text{Fe}$ or Mn) with the partial pressure of oxygen at 870°C .

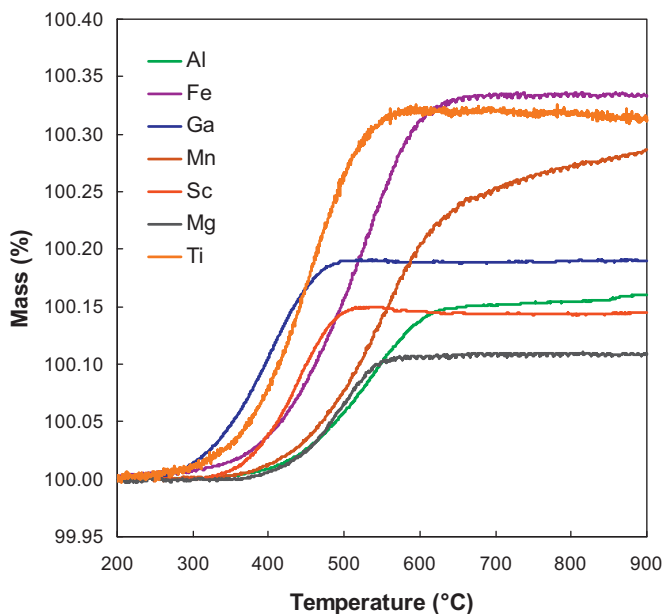


Fig. 2. Thermo-gravimetric analysis of the reoxidation of prereduced $\text{La}_4\text{Sr}_8\text{Ti}_{11}\text{XO}_{36+\epsilon}$ ($\text{X} = \text{Ti}, \text{Al}, \text{Ga}, \text{Fe}, \text{Mg}, \text{Mn}$ or Sc).

Al_2O_3 , Sc_2O_3 , iron oxalate dihydrate and TiO_2 (Aldrich) were mixed and ground in acetone in a planetary ball mills for 30 min. The powders were then calcined at 1250°C for 12 h. The resulting powder was then ground and pressed into pellets. These pellets were then placed in platinum crucibles and fired at 1500°C for 48 h. The pellets were then reground, pressed into pellets and refired under the same conditions.

Table 1
The change in mass and amount of oxygen recombined during reoxidation per perovskite unit.

X	Δm (%)	$n(\text{O})/\text{ABO}_3$
Al	0.16	0.020
Fe	0.34	0.043
Ga	0.19	0.024
Mg	0.11	0.014
Mn	0.31	0.039
Sc	0.14	0.018
Ti	0.31	0.039

X-ray diffraction (XRD) data were acquired using a STOE Stadi-P transmission X-ray diffractometer, using $\text{CuK}\alpha_1$ radiation in the range $2\theta = 10\text{--}90^\circ$ in steps of 0.1° at 30 s/step. The unit cells of the prepared materials were determined by standard least squares techniques available in the refinement modules of the Stoe software.

Thermo-gravimetric analyses of samples were carried out using a Netzsch STA 449 Jupiter instrument. Samples for reoxidation analysis were pre-reduced in 5% H_2 -Ar for 12 h at 900°C . Samples were heated to 900°C in oxygen at 5°C .

Four point conductivity measurements were performed using organo-platinum contacts pre-fired at 900°C . The surrounding atmosphere was varied between air and 5% H_2 in Ar to obtain conductivity data across range of oxygen partial pressures.

Fuel cell tests were carried out using the three-electrode setup, which consists of 1 cm^2 working and counter ring electrodes with a point electrode in the centre of the counter ring. The anodes for the fuel cell tests were applied as an ink to YSZ pellets of 2 mm thickness and 20 mm diameter. The ink was prepared by combining the compounds with 15 wt.% YSZ and 2 wt.% of KD1 dispersant (Uniqema) in acetone. To this slurry Johnson Matthey 63-2 screen vehicle was added in a ratio of 3 g to 10 g of solid and reground. The acetone was then allowed to evaporate until a suitable consistency was reached.

This was then fired at 1300°C for 2 h. Platinum paste was then applied to act as the cathode and a gold mesh current collector was attached to the working electrode by means of four small drops of gold paste. Before the fuel cell tests were carried out the anodes were left at 900°C in flowing 5% H_2 for 2 days to allow the anode materials to reduce in order to achieve the maximum conductivity.

The half cell tests were carried out using either humidified hydrogen (97% H_2 3% H_2O) or humidified methane (97% CH_4 3% H_2O) as fuels at the working electrode, while 100% O_2 was provided at the cathode. The impedance of the electrochemical cells was measured in the $10^6\text{--}0.1$ Hz frequency range, using an a.c. amplitude of 20 mV. The half cell performance was recorded by cyclic voltammetry.

3. Results and discussion

3.1. Structural characterisation

The as fired materials were yellow in colour, with the exception of the $\text{X} = \text{Mn}$ compound that was brown. Very small levels of Ti^{3+}

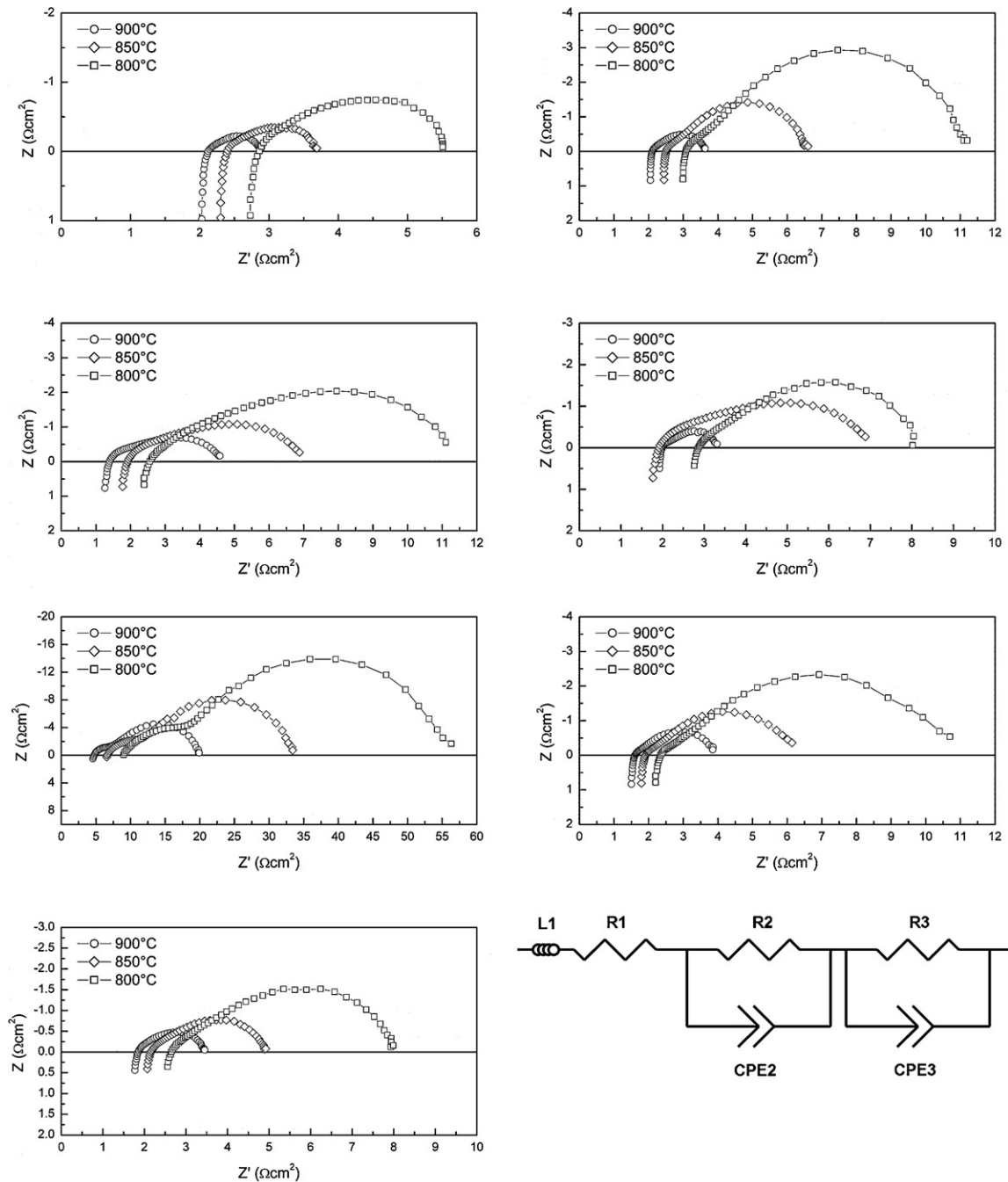


Fig. 4. Electrical impedance spectra of $\text{La}_4\text{Sr}_8\text{Ti}_{11}\text{XO}_{36+\epsilon}$ -8YSZ anodes in 97% H_2 -3% H_2O at 900 °C. (a) X = Ti, (b) X = Al, (c) X = Fe, (d) X = Ga, (e) X = Mg, (f) X = Mn, (g) X = Sc and (h) the corresponding equivalent circuit.

are known to turn strontium titanates black, indicating that the titanium ions in these compounds are almost all Ti^{4+} and that there is an oxygen over-stoichiometry. Additionally, other researchers who have prepared similar compounds by the same method and analysed the magnetic susceptibility have shown the as fired yellow compounds to be weakly paramagnetic and contain less than 1% Ti^{3+} [10].

The X-ray traces for the compounds $\text{La}_4\text{Sr}_8\text{Ti}_{11}\text{XO}_{36+\epsilon}$ are shown in Fig. 1. For the compounds X = Ti, Sc, Ga, Al and Fe the structure can be refined to the cubic perovskite structure, space group $Pm-3m$. For the X = Mg compound the structure was found to be distorted from simple cubic perovskite and instead has a rhombohedral structure, space group $R-3c$. The X = Mn compound can be refined to the cubic perovskite structure, however other studies using neutron diffrac-

tion show it to have the rhombohedral structure. This distortion is commonly observed in other lanthanum strontium titanates [6].

3.2. Thermo-gravimetric analysis

The redox behaviour of these compounds is strongly dependent on the nature of the dopant. The TGA results of the reoxidation of the compounds in oxygen, after reduction in 5% H_2 for 12 h at 900 °C, are shown in Fig. 2. Table 1 shows the corresponding change in mass and calculated number of moles of oxygen that are recombined per ABO_3 perovskite unit for each compound in Fig. 2.

It can be seen from the curves in Fig. 2 as well as the results in Table 1, that when titanium is replaced by a trivalent (Al^{3+} , Ga^{3+} and Sc^{3+}) or divalent (Mg^{2+}) ion the amount of oxidation decreases as

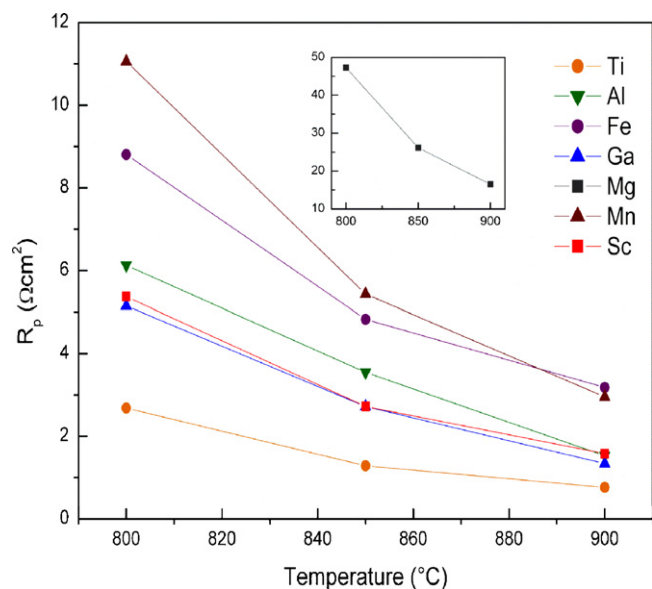


Fig. 5. The variation of polarisation resistance with temperature for all LSTX-YSZ anodes.

the charge on the dopant ion decreases. This is because the replacement of titanium with a single valency ion lowers the number of ions that can undergo reduction and subsequently reduces the mass gain on reoxidation. The use of the divalent Mg^{2+} ion as a dopant results in a compound that has the lowest amount of reoxidation. This is because the replacement of Ti^{4+} with Mg^{2+} leads to the greatest reduction in oxygen over-stoichiometry. This reduces the driving force for reduction. Similarly, when Ti^{4+} is replaced with a trivalent cation, as in the $X = Al^{3+}$, Sc^{3+} and Ga^{3+} compounds there is a once again a reduction in the amount of reducible species, Ti^{4+} and driving force for reoxidation, though not to the same extent as the case when $X = Mg^{2+}$.

In the case of the trivalent ions the temperature at which oxidation begins in these compounds varies as well as the amount of reoxidation, the $X = Ga$ compound begins reoxidation at $317^\circ C$, the Sc containing compound begins reoxidation at $366^\circ C$ and the $X = Al$ compound begins oxidation at $401^\circ C$. The gallium doped compound is the only compound analysed where reoxidation start temperature does not increase compared to the undoped compound. There is also variation in the amount of reoxidation the $X = Mg^{2+}$.

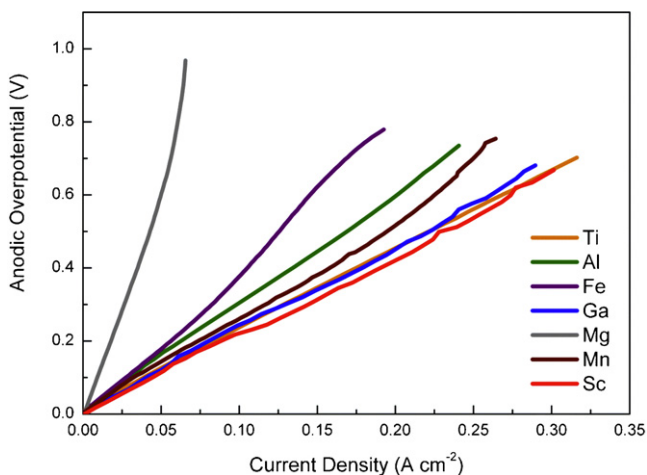


Fig. 6. Anodic overpotentials of $La_4Sr_8Ti_{11}XO_{36+e}$ -YSZ anodes operating in H_2 -3% H_2O at $900^\circ C$.

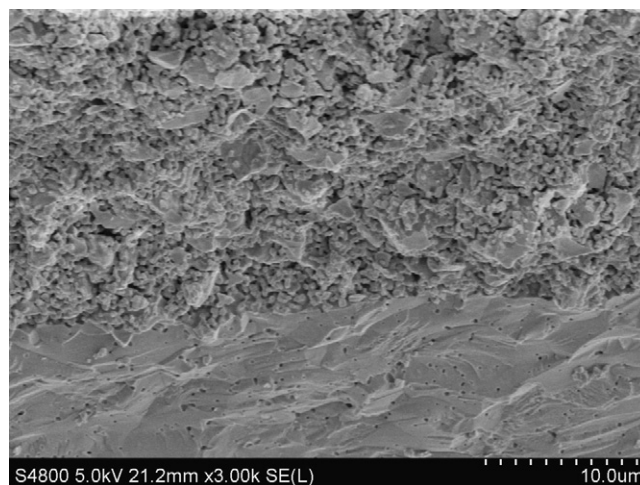


Fig. 7. Electrolyte anode interface in a fractured $La_4Sr_8Ti_{11}ScO_{36+e}$ -YSZ half cell.

doped compound regains 0.24 oxygen per perovskite unit compared to 0.20 and 0.18 per formula unit for Al and Sc respectively.

The behaviour of the compounds doped with the multivalent cations Mn and Fe varies significantly from the behaviour observed for the single valency cation doped compounds. For both the $X = Mn$ and Fe compounds the mass increase observed is greater than for the single valency doped compounds. The mass increase observed for the $X = Fe$ compound is very close to that observed for the undoped compound while the $X = Mn$ is the only compound that is still reoxidising when the temperature reaches $900^\circ C$. Initially the Mn doped compound oxidises rapidly from a start temperature of $400^\circ C$, however at around $650^\circ C$ the process slows and oxygen is absorbed at a slower rate as the temperature increases. One reason the amount of oxidation in these compounds is higher than in the compounds doped with single valency ions is that the titanium ions are being replaced by dopant ions that can also undergo reduction and reoxidation.

3.3. Electrical characterisation

Fig. 3 shows the conductivity of the $X = Al, Ga, Fe, Mn$ and Ti compounds as a function of the partial pressure of oxygen at $870^\circ C$. In all cases the gradients of the curves are negative and approach -0.166 or -0.25 indicating n -type conductivity. As well as the dopant cation the conductivity is also dependent on the microstructure and kinetic factors. The conductivities of the undoped $X = Ti$ compounds and the single valency cation doped $X = Al, Ga, Mg$ and Sc doped compounds range from 1.5 to $5.5 S cm^{-1}$ at an oxygen partial pressure of 10^{-18} . The higher conductivity of the Sc and Mg doped phases compared to the Al and Ga is due to improvements in experimental design that lead to the samples being exposed to more strongly reducing conditions resulting in slightly higher conductivities. The slower rate of the reoxidation reaction in the bulk material compared to the milled powder may prevent the true equilibrium conductivity being reached on reoxidation, giving higher values. In these compounds the charge carriers are provided by the reduction of Ti^{4+} to Ti^{3+} . A significant drop in conductivity is observed when the dopant is the multivalent Fe or Mn . Their conductivities at an oxygen partial pressure of 10^{-18} are only 0.6 and $0.15 S cm^{-1}$ respectively. These lower conductivities are most likely the results of the Fe and Mn ions being reduced in preference to the Ti ions as indicated by the TGA results.

The conductivities of these compounds are significantly less than the hundreds or thousands of Siemens per centimetre that could have been obtained were the compounds produced by fir-

ing at higher temperatures in reducing conditions. However it is also important that materials used in fuel cell manufacture do not irreversibly lose their high conductivity if exposed to an oxidising environment during operation or fuel cell processing. The lower conductivities obtained here are still high enough if these materials are used for their catalytic properties in a thin anode functional layer or in combination with other higher conductivity current collector compounds.

3.4. Half cell testing

The impedance results for the electrical half cell tests carried out at 900 °C in H₂-3% H₂O are shown in Fig. 4. The polarisation resistances versus temperature are shown in Fig. 5. In all cases the polarisation resistances were lower at higher temperatures. The lowest polarisation resistances are obtained for the X = Ti compound. Of the doped compounds the trivalently doped Sc and Ga gave the next lowest polarisation resistances followed by Al, Fe and Mn. The polarisation resistances of the Mg containing anode were significantly worse than the other anodes.

In each case the impedance spectrum can be fitted to the equivalent circuit shown in Fig. 4(h). The inductance, $L1$, and resistance, $R1$, are related to the inductance of the measurement setup and series resistance of the electrolyte and anode. The polarisation response of the anodes consisted of two arcs modelled by the resistances $R2$ and $R3$ and the constant phase elements CPE2 and CPE3. For each compound, the higher frequency $R2$ -CPE2 arc has a low CPE exponential of 0.5 or lower, and an activation energy of around 1.1 eV. This is indicative of a diffusion related process. The $R3$ -CPE3 element has higher capacitances and activation energy of 1.5 eV. This is consistent with for example a Ti(IV) to Ti(III) redox couple. This may indicate that the cyclic reduction and oxidation of the oxide, as oxygen ion and electrons are transferred, may be playing an important electrocatalytic role in the anodic reaction.

Fig. 6 shows the over-potential versus current density curves corresponding to the anodes in Fig. 4 at 900 °C. As expected from their comparatively high polarisation resistances the performance of the X = Mg and Fe compounds are low compared to the other compositions. The X = Ti, Al, Ga, Mn and Sc all showed similar performance at low over-potentials with differences only becoming apparent at higher currents. The X = Mn anode performed better than would be expected from its high polarisation resistance. A reduction in polarisation resistance was observed when the anode was under load compared to at open cell potential.

Numerous studies have shown the importance of microstructure on fuel cell anode properties. The performance of an anode is a complex function of many factors that include particle size, electrical conductivity, ionic conductivity, triple-phase boundary length, surface area and pore volume and tortuosity. Fig. 7 shows the microstructure of the anode for the X = Sc compound. Similar microstructures were observed for all compositions. The anode

can be seen to consist of fine sub micrometre particles and larger angular micrometre sized particles. Microstructural effects are the likely cause of the unexpectedly low series resistance of the Mn and Fe containing anodes. The Mn and Fe containing titanates exhibit higher resistivities than the other compounds, yet their anodes showed lower series resistances. This is likely the result of microstructure effects. Small differences in microstructure due to changes in sintering response may have lead to a denser and higher percolation of the electronically conducting titanate throughout the anode. Further studies involving more fundamental characterisation of these compounds and/or the microstructural optimisation of lanthanum strontium titanium based anodes should lead to a greater understanding of the role of microstructure on electrocatalytic properties.

4. Conclusions

The effect of B-site doping has been analysed on the series of perovskite compounds, La_{0.67}Sr_{0.33}Ti_{0.92}X_{0.08}O_{3+δ}, where X = Ti, Al, Fe, Ga, Mg, Mn and Sc. The compounds were shown to have perovskite average structure. The redox properties and conductivity of the compounds are both also strongly influenced by the choice of dopant. Varying the choice of dopant affects both the amount of reduction/reoxidation as well as the reoxidation kinetics. In undoped and single valency cation doped compounds changes in oxidation state that accompany reduction/reoxidation only involves titanium cation. In compounds containing the multivalent manganese and iron cations, these species undergo the reduction and oxidation as well or in preference to the titanium. Because less Ti(IV) is reduced to Ti(III) in the iron and manganese doped compounds they have lower conductivity. Half cell testing of these compounds shows they have some electrocatalytic activity, though optimisation of the microstructure may lead to improved anode performance

References

- [1] O.A. Marina, N.L. Canfield, J.W. Stevenson, *Solid State Ionics* 149 (2002) 21–28.
- [2] J. Canales-Vazquez, *Studies on Oxygen Excess Perovskite-Based Titanates for SOFC Fuel Electrodes*, Ph.D Thesis, School of Chemistry, University of St Andrews, 2003.
- [3] D.P. Fagg, et al., *J. Eur. Ceram. Soc.* 21 (2001) 1831–1835.
- [4] X. Huang, et al., *J. Phys. Chem. Solids* 67 (2006) 2609–2613.
- [5] O.A. Marina, L.R. Pederson, 5th European Solid Oxide Fuel Cell Forum, Lucerne, Switzerland, 2002.
- [6] A. Ovalle, et al., *Solid State Ionics* 177 (2006) 1997–2003.
- [7] J.C. Ruiz-Morales, et al., *Nature* 439 (7076) (2006) 568–571.
- [8] L. Yang, et al., *J. Electrochem. Soc.* 154 (9) (2007) B949–B955.
- [9] J. Canales-Vazquez, S. Tao, J.T.S. Irvine, *Solid State Ionics* 159 (2003) 159–165.
- [10] J. Canales-Vázquez, et al., *Adv. Funct. Mater.* 15 (2005) 1000–1008.
- [11] J. Canales-Vázquez, et al., *J. Electrochem. Soc.* 152 (7) (2005), A1558–A1465.
- [12] M.J. Escudero, J.T.S. Irvine, L. Daza, *J. Power Sources* 192 (2009) 43–50.
- [13] J. Ruiz-Morales, et al., *Solid Oxide Fuel Cells*, 10, The Electrochemical Society, Nara, Japan, 2007.